

## Dynamics of Macropore Growth in n-type Silicon Investigated by FFT In-Situ Analysis

J. Carstensen, A. Cojocaru, M. Leisner, and H. Föll

Institute for Materials Science, University of Kiel, Kaiserstrasse 2, 24143 Kiel, Germany

The dynamics of macropore growth in n-type silicon were investigated by in-situ FFT impedance spectroscopy and transient analysis. In particular the response to fast growing pores to current density steps in the context of so-called anti-phase diameter oscillations was investigated. These pore growth mode allows for a very fast growth of deep macropores and could for the first time be stimulated by external current steps.

### Introduction

Since the discovery of macropore formation in n-type Si with backside illumination (bsi) by Lehmann and Föll (1), many investigations have been undertaken with the aim to obtain a good understanding of the underlying phenomena, cf. (2 - 4). As a result a very good control of pore geometries emerged, even for extremely deep pores; although some puzzling details remained, like the slow nucleation of macropores without lithographically pre-structured nucleation sites (5, 6), or the non-linear response of the pore diameter to modulations of the current density (7). Moreover, fast etching with high HF concentrations and correspondingly high current densities to large depths (8) produced unexpected results, in particular self-induced anti-phase diameter oscillations as shown in **Fig. 1**, often preceded and followed by several further growth mode transitions (9). This indicates that pore formation at high etching rates (and to some extent also at low etching rates / current densities) is dominated by kinetics, i.e. rate limiting time constants.

In order to investigate the underlying processes causing growth mode transitions a combination of impedance analysis and transient analysis is used in this paper. While impedance analysis, i.e. the linear response analysis of the system to a sinusodially modulated perturbation, is efficient for fast processes, it becomes very time consuming for slow processes, since an average over several oscillation periods is needed to gain a good signal to noise ratio. In contrast, transient analysis (response of the system to a step-like change of a parameter) is better suited for a reliable analysis of time constants of slow processes, since the determination of a relaxation time needs only a (large) number of measured points within a period of 3 to 4 times the relaxation time after the step and this can be done with a small sampling rate. In contrast, for fast processes a large sampling rate would be needed leading to correspondingly large errors in the measured data.

In the experiments reported here the etching current density (controlled by the backside illumination) is changed step-like with various period lengths after the macro pores have reached a certain depth.

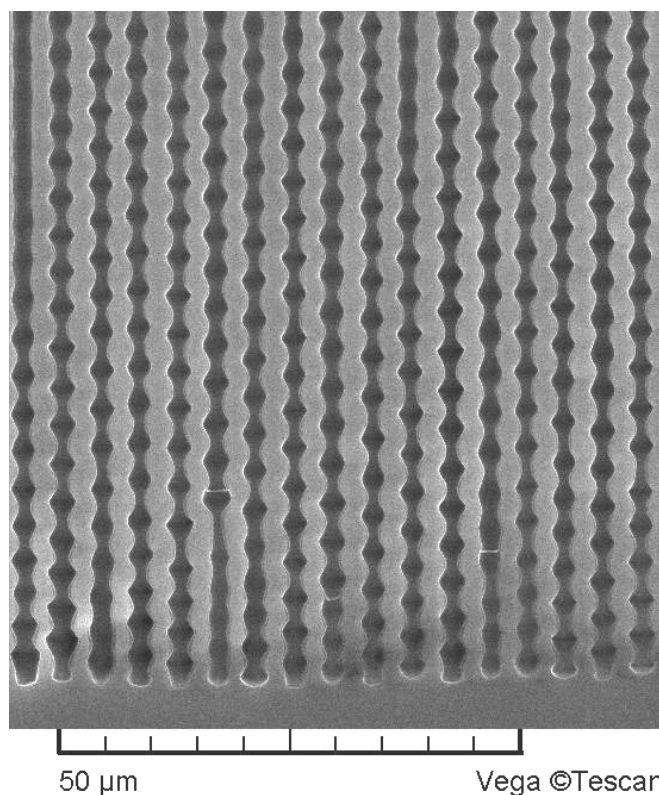


**Fig. 1:** Self-induced “anti-phase” pore diameter oscillations in macropores in n-type Si.

This allows to investigate the slow transient processes and to check if and under which conditions anti-phase pore diameter oscillations can be triggered by external current stimuli. Simultaneously the voltage and illumination impedance (c.f. (8, 10)) are measured every 2 to 3 seconds to monitor the (fast) electrochemical processes.

### Experimental Details

Low doped ( $5 \Omega\text{cm}$ ) (100) oriented n-type Si wafers with an  $n^+$  layer on the back side for good ohmic contact were etched at a controlled temperature of  $20^\circ\text{C}$ . The samples were pre-structured by standard photolithography; the nucleation pattern was a hexagonal lattice with a lattice constant of  $a = 4.2 \mu\text{m}$ . The electrolyte consisted of 15 wt.% HF in an aqueous-viscous solvent. Carboxymethylcellulose sodium salt (CMC) was added to the electrolyte (0.42 g/l) to increase the viscosity. The pores are etched using the basic parameters taken from the “Lehmann model” (2), i.e. the initial current density  $j(t)$  and its decrease with time was chosen to yield pores with  $2 \mu\text{m}$  diameter. To investigate the bsi pore formation kinetics *in-situ* FFT impedance spectroscopy (11) has been used. The current density  $j(t)$  started at  $27 \text{ mA/cm}^2$  and was reduced as a function of time to compensate for the reduction of the electrolyte concentration at longer pore tips, e.g. to  $24 \text{ mA/cm}^2$  after 10 min. Current steps with periods of 1 min, 2 min, and 5 min were applied in which the current was lowered by a factor of two of  $j(t)$ . The number of steps started from one and two up to 70.

The FFT impedance spectrometer was embedded within the etching system (ET&TE GmbH) and was used to extract in-situ information concerning the pore etching. The impedance measurements were performed at intervals of 1 second in a frequency range between 100 Hz and 20 kHz, containing 27 frequencies.

## Results and Discussion

**Fig. 1** shows the self-induced anti-phase diameter oscillations obtained with electrolytes of high HF concentration ( $c_{\text{HF}} \gg 5 \text{ wt\%}$ ) and correspondingly high current densities. The period of the pore diameter oscillation can be estimated from the pore growth speed and the distance of two diameter maxima to be in the order of minutes. To investigate the etching conditions that allow for such anti-phase diameter oscillations, etching current steps were applied to the etching process. **Fig. 2** shows the SEM images of applying just one step by reducing the current density by a factor of two for 1 min. and 2 min., respectively, and afterwards continuing the experiment with the original current density. Neither in **Fig. 2a** (step of 1 min.) nor in **Fig. 2b** (step of 2 min.) diameter modulations in the following high current density phase are found, i.e. growth mode transition leading to self-sustained oscillations could be triggered. While the current density is reduced, only a decrease of the pore diameter is found. The diameter decreases by about  $1.43 \approx \sqrt{2}$  as is expected from the Lehmann model, which predicts a change of pore tip area by a factor of two, i.e. a factor  $\sqrt{2}$  for the pore diameter. In addition, for the 2 min. step the first stage of cavity formation is found soon after the current density has been increased to the full value again, but not for the 1 min. step. Such cavities are always found for the etching condition discussed here (cf. (8)), terminating the pore growth, but typically at larger pore depth. Since the cavity formation is related to strong diffusion limitation this is a first hint that the “bottle neck” induced by the current step already leads to a significantly increased diffusion limitation.

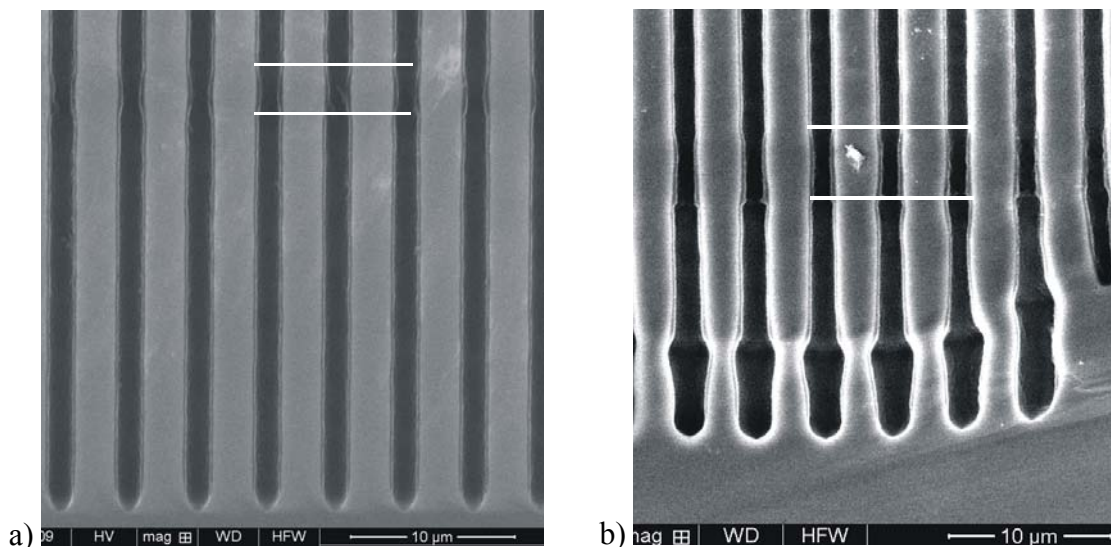


**Fig. 2:** SEM cross section of macropores. After 5 min. a current step with a period of a) 1 min. and b) 2 min. was initiated. The white lines indicate the region of reduced diameter.

**Fig. 3** shows the pores when 2 current density steps were applied. In **Fig. 3a** (step time 1 min.) the diameter reduction as already seen in **Fig. 2a** is now found twice. In contrast to this, in **Fig. 3b** (step time 2 min.) anti-phase diameter modulations are visible. These anti-phase diameter modulations are obviously induced by the current density steps since under these etching condition *self-induced* anti-phase diameter modulation do not exist. As soon as the current density is constant again the diameter modulations stop as well (and cavity formation starts). Anti-phase diameter modulations thus are not yet

stable under the applied etching condition, even if they are induced externally. This is reminiscent, to some extent, to the triggering of current oscillations in Si in a region of parameter space where these oscillations are possible but heavily damped (12).

Stable self induced anti-phase diameter oscillations occur at larger pore depths and lower current densities. The triggering of the anti-phase diameter modulation apparently needs the right period for the current steps. While it does not work for a period of 1 min. as shown in **Fig. 3a**, it does work for a period of 2 min. (**Fig. 3b**) and also for a period of 5 min. (not shown here). However, applying a step of 2 min. to pores that are significantly longer, i.e. later in the process, anti-phase diameter modulations cannot be induced. This indicates that there is only a limited region in parameter space where anti-phase diameter oscillations “resonate” with external stimuli as shown in **Fig. 2b**. Alternatively, some kind of feedback might be required to find the proper period and the modulation amplitude of the current density as a function of pore depth.

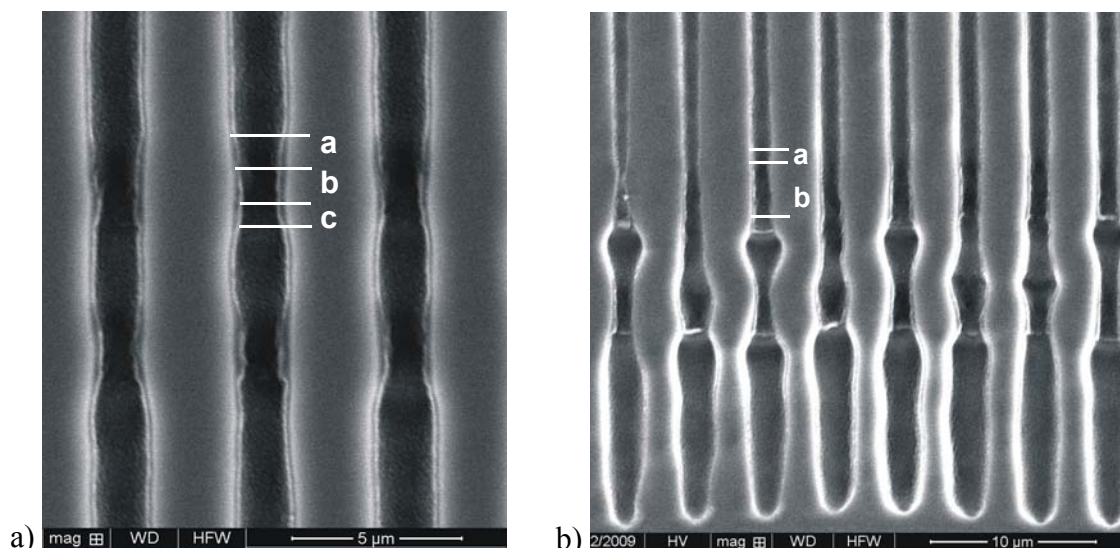
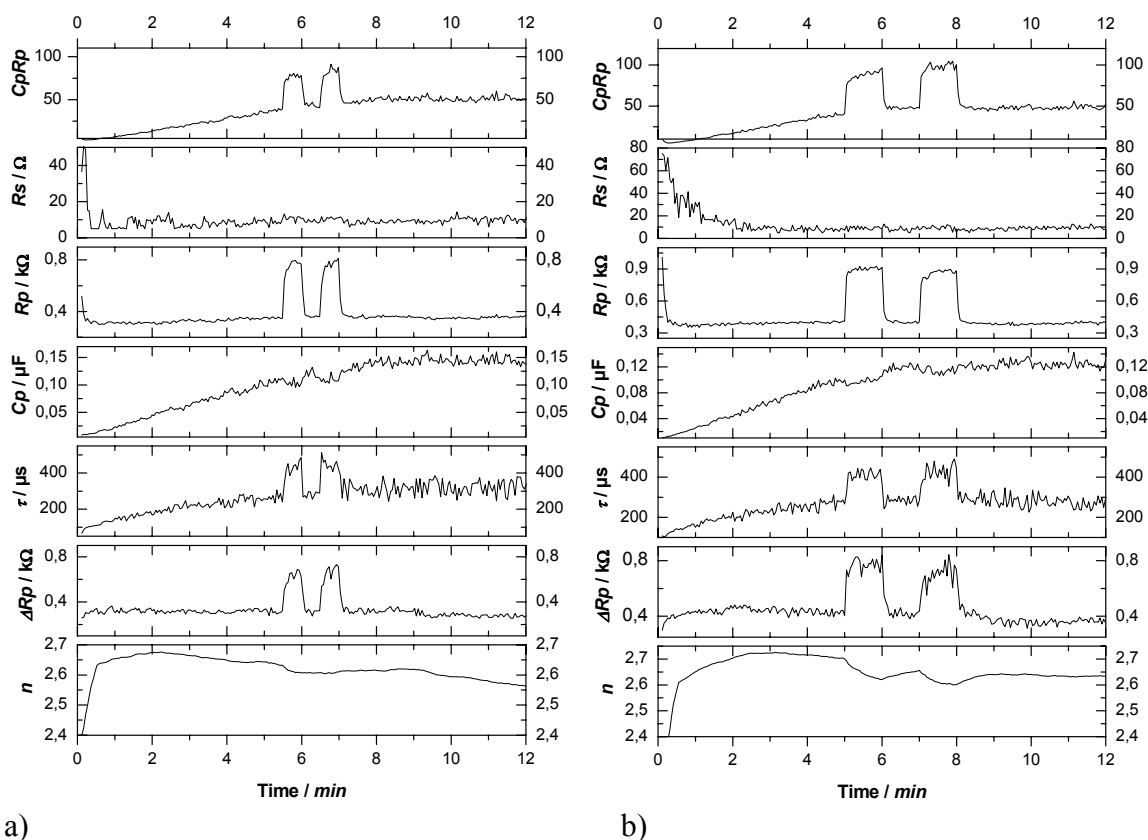


**Fig. 3:** SEM cross section of macropores. After 5 min. the current was modulated stepwise two times with different periods: a) 1 min. and b) 2 min. The white lines indicate the borders of regions described below and in **Fig. 5**.

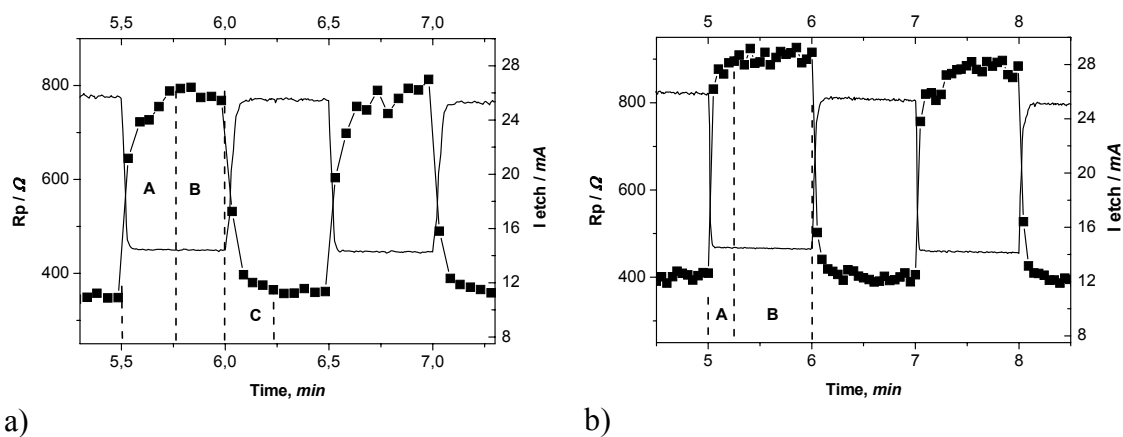
To get in-situ information about the etching processes and thus also for a possible feedback for controlling the anti-phase diameter oscillations, in-situ FFT impedance analysis was performed for the whole time of all experiments. In this case only voltage impedance was used; the data obtained were analyzed using a model that allows for a very good fit of all impedance data for nearly all types of macropores formed by using backside illumination (8, 10). The most relevant parameter of the model in the context of this paper is the transfer resistance  $R_p$  that essentially describes the chemical dissolution process. The impedance results for the etching of the pores shown in **Fig. 3** are displayed in **Fig. 4**. **Fig. 4a** shows the model parameters as a function of time for the 1 min. steps and **Fig. 4b** for the 2 min. steps.



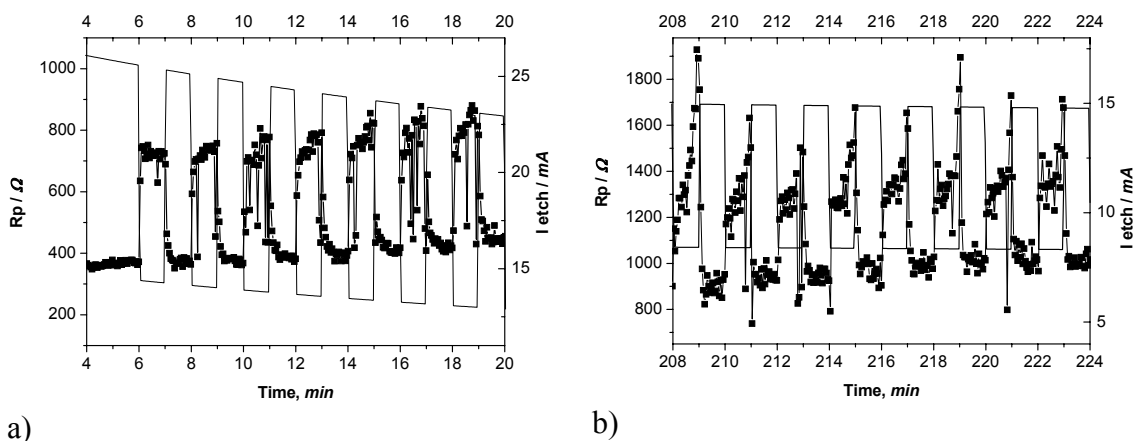
a) b)  
**Fig. 4:** The model parameters as obtained from the fit of the impedance data for the macropores presented in **Fig. 3**. Two current steps were used with different periods of a) 1 min. and b) 2 min.

While the series resistance  $R_s$  and the interface capacitance  $C_p$  do not change significantly when changing the current density, strong changes are found for the time constants  $C_p R_p$  and  $\tau$  and the transfer resistances  $R_p$  and  $\Delta R_p$ . The time constants  $C_p R_p$  and  $\tau$  show a significant dependence on time, resp. pore length, while the transfer resistances  $R_p$  and  $\Delta R_p$  are nearly independent of pore depth. Since the noise in  $R_p$  is much smaller than the noise in  $\Delta R_p$  and the changes in the transfer resistance  $R_p$  are most easily understood; a detailed view is shown in **Fig. 5** (note the factor 2 in the scaling of the time axis).

$R_p$  should scale inversely proportional to the integral pore tip area, i.e. the actively etched area. In the case of n-macro(bsi) pores the etched area is the sum of all macropore tips, which under perfect conditions is proportional to the current density. **Fig. 5a** and **Fig. 5b** both show an increase of  $R_p$  by roughly a factor of two after reaching steady state between the phases of high current density and of low current density. This is in good agreement to the measured decrease of the pore tip areas of a factor of two. Steady state is reached for both experiments after roughly 0.5 min.; this is marked by dotted lines that separate the areas "A" and "B" in **Fig. 5a** and **Fig. 5b**. A very good agreement to the corresponding areas in **Fig. 3** is found: The horizontal lines mark the start point and the end point of the areas "a" to "c" in **Fig. 3**. A nearly linear transition from large pore diameter to small pore diameter is found. The areas "a" and "b" in **Fig. 3** correspond to the areas "A" and "B" in **Fig. 5**.



a) b)  
**Fig. 5:** Details of the transfer resistance  $R_p$  as presented in Fig. 4.



a) b)  
**Fig. 6:** The impedance parameter  $R_p$  for an experiment with 70 steps with a period of 2 min. a) Beginning of the experiment; b) near the end of the experiment.

Since the length for  $(a+b)$  in both images in Fig. 3 is the same, and taking into account the factor of 2 in the magnification between Fig. 3a and Fig. 3b, one can state that the pore growth speed in both cases is the same. The length of the bottle neck in Fig. 3b is twice as long as that in Fig. 3a, but the transition pore length from large to small diameter in both cases is the same. Therefore the ratio between the transition pore length and the pore length with steady state condition changes from 1 in Fig. 3a to 4 in Fig. 3b. The same ratios are found for the periods of area "A" and area "B" in Fig. 5a and Fig. 5b. Obviously this larger time for steady state in the phase of low current density is necessary to stimulate the anti-phase diameter modulation.

Already for the second current density step a significant increase in the transient time is found in Fig. 5a as well as in Fig. 5b. The transient time changes substantially as a function of pore depth; this is shown in Fig. 6a for  $R_p$  at the beginning of the experiment and in Fig. 6b for the end of the same experiment where current density steps of 2 min. period for more than 200 min. Obviously the transient time needed for the etching system to adapt to the lower or higher current densities, resp., drastically increases as a function of pore length.

Summing up the results the anti-phase diameter modulation could only be induced after 5 min. of pore etching by 2 current steps with a period of 2 min. Neither a period of 1 min. nor a period of 5 min. allowed for a stimulation. Neither staying at low current density nor staying at high current density after the two steps allowed for a continuation

of the induced anti-phase growth. So in this experiments only a period of 8 times the transient time allowed for a stimulation of the anti-phase diameter modulation growth. Applying two current density steps with a period of two minutes much later in the experiment did not allow for the stimulation as well. This implies that the correct duration for applying low current densities and for applying high current densities is necessary. Staying for a too long time at high current densities cavity formation will occur. Staying for a too long time at low current densities several pores will stop growing while the remaining pores start to branch heavily.

The anti-phase diameter growth allows for an optimal current density of  $J_{psl}$  (as assumed by the Lehmann model) while the pore tip is growing and for the necessary time for recovering the electrolyte concentration while the pore tip is not growing, i.e. the neighboring pores consume the hole generated by backside illumination. If some pores completely stop to grow the distance between neighboring pores increases which is not optimal since the distance should coincide with the width of the space charge region around the pores.

To stimulate and stabilize the anti-phase diameter modulation could therefore be a promising way for growing deep macropores with the highest possible growth rates. As mentioned above, this probably needs some kind of feedback to control the modulation period. Summarizing the results of this paper a possible algorithm using the information of the FFT impedance analysis may be:

1. Start a step like modulation when a reasonable pore depth has been reached (possibly controlled by in situ impedance analysis as well).
2. Extract the relaxation  $\tau$  time from the analysis of the transient e.g. of  $R_p$ .
3. Chose a step period time  $t = x \tau$  where  $x$  is a constant (probably optimized by a series of experiments).

The near future will show, if this algorithm allows for the expected stable and fast macropore growth.

## References

1. V. Lehmann and H. Föll, *J. Electrochem. Soc.* **137**, 653 (1990).
2. V. Lehmann, *Electrochemistry of Silicon*, Wiley-VCH, Weinheim (2002).
3. X.G. Zhang, *J. Electrochem. Soc.* **151**, C69-C80 (2004).
4. C. Fang, J. Carstensen, and H. Föll, *Solid State Phenomena* **121-123**, 37 (2007).
5. M. Hejjo Al Rifai, M. Christophersen, S. Ottow, J. Carstensen, and H. Föll, *J. Porous Mater.* **7**, 33 (2000).
6. M. Hejjo Al Rifai, M. Christophersen, S. Ottow, J. Carstensen, and H. Föll, *J. Electrochem. Soc.* **147**, 627 (2000).
7. S. Matthias, F. Müller, J. Schilling, and U. Gösele, *Appl. Phys. A* **80**, 1391 (2005).
8. A. Cojocar, J. Carstensen, M. Leisner, H. Föll, and I.M. Tiginyanu, *Phys. Stat. Sol. (c)*, in print (2008).
9. J. Carstensen, A. Cojocar, M. Leisner, and H. Föll, *ECS Trans.* **16**, 21 (2008).
10. A. Cojocar, J. Carstensen, and H. Föll, *ECS Trans.* **16**, 157 (2008).
11. J. Carstensen, E. Foca, S. Keipert, H. Föll, M. Leisner, and A. Cojocar, *Phys. Stat. Sol. (a)* **205**, 2485 (2008).
12. E. Foca, J. Carstensen, and H. Föll, *J. Electroanal. Chem.* **603**, 175 (2007).